

Kaleidoscope modes in large aperture Porro prism resonators

Liesl Burger^{1,2,*} and Andrew Forbes^{1,2†}

¹CSIR National Laser Centre, PO Box 395, Pretoria 0001, South Africa

²School of Physics, University of KwaZulu-Natal, Private Bag X54001, Durban 4000, South Africa

Corresponding authors: *lburgerl@csir.co.za, †aforbesl@csir.co.za

Abstract: We apply a new method of modeling Porro prism resonators, using the concept of rotating loss screens, to study stable and unstable Porro prism resonator. We show that the previously observed petal-like modal output is in fact only the lowest order mode, and reveal that a variety of kaleidoscope beam modes will be produced by these resonators when the intra-cavity apertures are sufficiently large to allow higher order modes to oscillate. We also show that only stable resonators will produce these modes.

©2008 Optical Society of America

OCIS codes: (140.4780) Optical resonators; (260.0260) Physical optics; (140.3410) Laser resonators; (230.5480) Prisms; (140.0140) Lasers and laser optics.

References and Links

1. B. A. See, K. Fuelop, and R. Seymour, "An Assessment of the Crossed Porro Prism Resonator," Technical Memorandum ERL-0162-TM, Electronics Research Lab Adelaide (Australia) (1980).
2. M. Henriksson, L. Sjöqvista, and T. Uhrwing, "Numerical simulation of a battlefield Nd:YAG laser," Proc. SPIE **5989**, 59890I (2005).
3. M. Henriksson and L. Sjöqvist, "Numerical simulation of a flashlamp pumped Nd:YAG laser," Report # ISRN FOI-R-1710-SE, Swedish Defence Research Agency, Linköping, Sensor Technology (2007).
4. M. Ishizu, "Laser Oscillator," US Patent 6816533 (2004).
5. A. Rapaport and L. Weichman, "Laser Resonator Design Using Optical Ray Tracing Software: Comparisons with Simple Analytical Models and Experimental Results," IEEE J. Quantum Electron. **37** 1401–1408 (2001).
6. I. A. Litvin, L. Burger, and A. Forbes, "Petal-like modes in Porro prism resonators," Opt. Express **15**, 14065–14077 (2007).
7. N. Hodgson and H. Weber, *Laser Resonators and Beam Propagation: Fundamentals, Advanced Concepts and Applications* (Springer, 2005), Chap. 20.
8. W. Liu, Y. Huo, X. Yin, and D. Zhao, "Modes of Multi-End-Pumped Nonplanar Ring Laser," IEEE Photonics Technol. Lett. **17**, 1776–1778 (2005).
9. C. Bollig, W. A. Clarkson, D. C. Hanna, D. S. Lovering, and G. C. W. Jones, "Single-frequency operation of a monolithic Nd:glass ring laser via the acousto-optics effect," Opt. Commun. **133**, 221–224 (1997).
10. Z. Bouchal, "Nondiffracting optical beams: physical properties, experiments, and applications," Czech. J. Phys. **53**, 537–624 (2003).
11. M. Anguiano-Morales, A. Martinez, M. D. Iturbe-Castillo, and S. Chavez-Cerda, "Different field distributions obtained with an axicon and an amplitude mask," Opt. Commun. **281**, 401–407 (2008).

1. Introduction

Porro prisms have the useful property that all rays incident on the prism are reflected back parallel to the initial propagation direction, independent of the angle of incidence, thus making them insensitive to misalignment. This property is used in a Porro prism resonator, in which the end mirrors of a simple flat-flat resonator have been replaced by Porro prisms. Such resonators have been exploited for their ruggedness, and found use in applications where a laser beam is required at a large distance from the source, and where the source is not a stable platform; for example, range finding and laser designators, mostly for the military [1–4]. Comprehensive models of these resonators exist [2,3,5], and have considered gain and output coupling loss, polarization, stability and temporal behavior, but despite the ubiquitous nature

of these lasers in the field, for a long time the output spatial modes from such lasers were not fully understood. Recently a new approach to modeling Porro prism resonators has been outlined, making use of rotating loss screens to mimic intracavity Porro prisms, which correctly predicts all the salient features of the observed petal-like spatial modal patterns [6].

In this paper we apply the model in [6] to stable and unstable Porro prism resonators with large intracavity apertures. In section (2) we briefly review the conditions under which petal-like modes are found. In section (3) we consider large aperture stable resonators, and show that higher order modes exist and can be made to resonate if the intracavity apertures are sufficiently large. Further we make use of non-planar, unidirectional resonance analysis [7–9] to understand the oscillating modes supported in these resonators (section (4)). These higher order modes bear close resemblance to recently reported kaleidoscope modes [10,11]. In [10] the kaleidoscope modes were generated external to a laser cavity using a loss screen with remarkable similarity to that found inside stable Porro prism resonators. These similarities and the implications thereof are discussed in section (5). This leads to the conclusion, in section (6), that the petal-like modes hitherto reported are in fact only the lowest order modes, while higher order kaleidoscope modes are possible given sufficient transverse spatial extent to oscillate.

2. Porro prism resonator model

We followed the approach to modeling Porro prism resonators detailed in [6], but briefly review the salient facts here to enhance clarity and readability of the paper. To build a physical optics model of a typical Porro prism resonator (see Fig. 1), the prisms are modeled as mirrors with rotating loss screens.

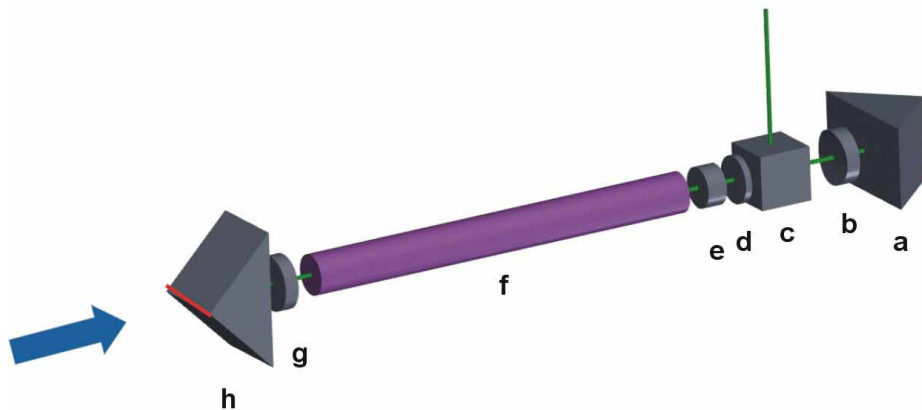


Fig. 1. A typical Porro prism based Nd:YAG laser with passive Q-switch, showing the following optical elements: Porro prisms (elements a and h); intra-cavity lenses (elements b and g); a beamsplitter cube (element c); a quarter wave plate (element d), and a passive Q-switch (element e). The prism apexes are shown in red.

This leads to a discrete set of Porro angles – the angle between the apexes of the opposite prisms when the prisms are viewed along the resonator length (direction of blue arrow in Fig. 1) – that allow the rotating loss screens to repeat on themselves, a necessary condition to generate the petal-like modes. At these discrete angles, α , the oscillating field is sub-divided into a finite number (N) of petals, given by:

$$N = \frac{j2\pi}{\alpha} \quad (1)$$

where

$$\alpha = \frac{i\pi}{m}, \quad (2)$$

and i, j , and m are integers, with certain constraints placed on j [6]. The combination of allowed Porro angles and associated number of petals is illustrated in Fig. 2(a) together with examples of the petal-like modes (Fig. 2(b)) commonly observed from Porro resonators.

The Porro prism resonator investigated in this study was based on the system shown in Fig. 1, with an optical path length from prism to prism of $L = 10$ cm, and lasing at $\lambda = 1064$ nm. Two Porro prisms at either end of the laser formed the resonator, replacing traditional mirrors. The stability of the resonators was determined by the two identical intra-cavity lenses (of focal length f) each placed adjacent to a prism. The resonator was confined in the transverse direction by circular apertures placed immediately in front of each prism, and with radius a .

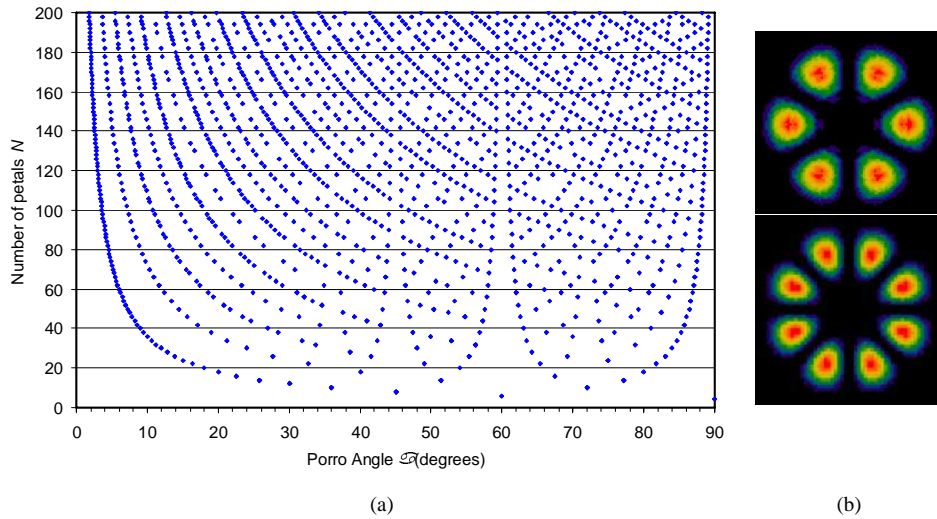


Fig. 2. (a) Plot of the discrete set of angles α that give rise to a petal pattern, with the corresponding number of petals to be observed; (b) example of petal-like modes for $\alpha = 60^\circ$ (top) and $\alpha = 45^\circ$ (bottom).

The laser was modeled by successive passes through a folded-out resonator without any gain, using an array size of 1024×1024 to describe the oscillating field. The modal build-up was started from a field comprising random noise, and continued until the round trip loss stabilized to within 0.5%. Each prism was assumed to be equivalent to a perfect mirror superimposed on a rotating loss line as described in [1].

3. Generalized modal patterns

In this section we vary both the lens focal lengths f , and the aperture radius a in order to investigate the impact of resonator stability and effective Fresnel number on the oscillating modes. Because of the symmetry of the lens-aperture configuration, any chosen stable resonator can be described in terms of just two parameters:

$$G = g_1 = g_2 \quad (3)$$

and

$$N_F = \frac{a^2}{\lambda L} \quad (4)$$

Here G is the equivalent G -parameter of the resonator, and N_F is the effective Fresnel number; λ denotes the wavelength of the laser light in vacuum and L is the total optical path length inside the resonator.

The first observation is that unstable resonators do not generate repeating petal-like patterns, while stable resonators do. We preempt our discussion to follow later with the following geometrical optics argument: a ray traversing the resonator must return to a loss-free sub-division in order to create the complete petal pattern. The lack of ray repeatability and confinement in an unstable resonator precludes this from happening, and hence only stable resonators exhibit the petal-like modes. We can further eliminate loss as a mechanism to explain this observation in that the loss for both stable and unstable resonators was set arbitrarily in this study and yet did not influence the observation of petals, or the lack thereof. The discussion to follow will therefore concentrate on stable resonators only. Without any loss of generality, all spatial modes to follow are calculated at the face of one of the Porro prisms, and may be propagated to any other plane if so desired.

Consider by way of example three stable resonators chosen so that $G = 0.75$ and with Porro angles (α) of 60° , 45° and 30° respectively. When the intracavity aperture is very small ($N_F \sim 1.5$), no mode is able to resonate. At intermediate aperture sizes ($N_F \sim 3.5$) the conventional petal-like modes are observed, with 6, 8 and 12 petals for $\alpha = 60^\circ$, 45° and 30° respectively. At large aperture sizes ($N_F > 6$) the petal-like modes give way to more complex mode patterns. This increase in mode complexity as the aperture size increases suggests that the petal-like modes are in fact the lowest order modes of Porro prism resonators, while previously unreported higher order modes also exist, and can be made to resonate if given sufficiently large transverse freedom. These results are shown in Fig. 3.

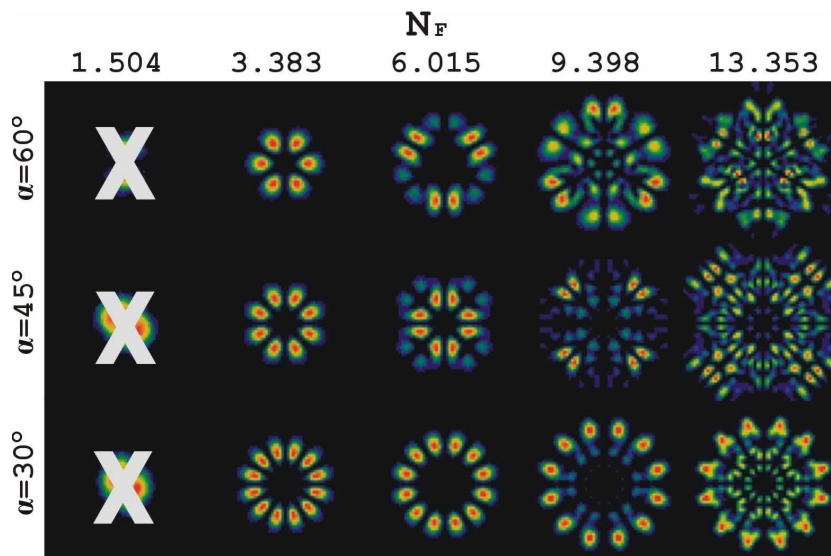


Fig. 3. Modal patterns for the three Porro angles with increasing effective Fresnel number to the right in each row. As N_F is increased (through an increase in aperture size), the modes become more complex, departing from the petal-like standard. ([Media 1](#)), ([Media 2](#)), ([Media 3](#)).

Porro prism resonators appear to offer a rich landscape of possible modes, many of which have not been associated with this type of resonator previously. While the previous discussion focused on one particular resonator for three Porro angles, we illustrate in Fig. 4 that the resonator parameter G also influences the oscillating mode, as one might expect.

While the results are illustrated for $\alpha = 45^\circ$, similar results are found at other Porro angles.

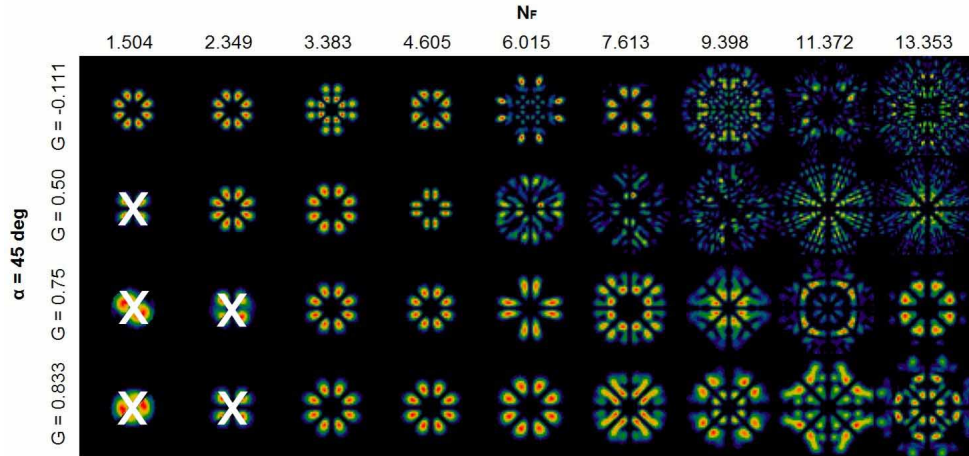


Fig. 4. The output modes of a number of Porro prism resonators arranged as a function of G (rows) and N_F (columns). Note that in the petal-like cases the single repeating mode is shown, while in the higher order mode cases, only one of the oscillating modes is shown (Media 4).

4. Mode periodicity

The higher order modes depicted in Fig. 3 and Fig. 4 exhibit an interesting feature: they repeat after a fixed number of passes through the resonator. This periodicity is not a function of the Porro angle α but rather of G , and is the result of the resonator's complex eigenvalues. One can understand this periodicity if one considers the similarities to the well-known Herriot cell resonator [7] and by following the path of a ray through the resonator. Such resonators result in a periodicity that is not a double pass through the resonator, as is the case in a standard Fabry-Perot system, but rather is based on a uni-directional analysis, where the number of passes can be made very large for a complete "round trip" – in this case "round trip" refers to the condition that the beam repeats a previous path through the resonator. The number of reflections and the orientation of the beam, and hence the periodicity of the resonator, can be controlled by judicious choice of the resonator parameters. This concept is illustrated in Fig. 5 where a standard resonator is operated as a non-planar ring laser [8]. In this case the beam passes through the resonator six times (or reflects off each mirror three times) in a single "round trip".

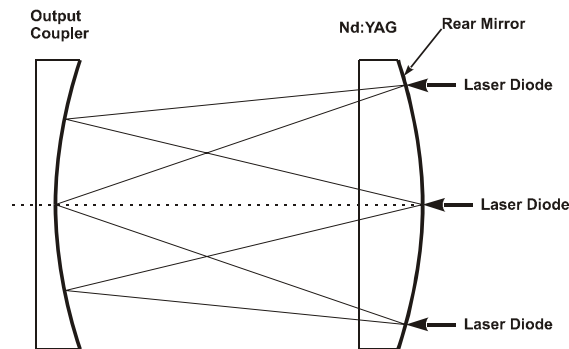


Fig. 5. A multi-pass beam pass is possible for a given resonator configuration. If the gain region is small and central then a Gaussian mode is expected. The resonator can be forced into a higher multi-pass mode by off-centre pumping.

Such a configuration leads to a complex output beam pattern based on the possible beam paths through the resonator, which we can refer to as beam loops. Since each beam loop has a

particular output pattern, it is convenient to refer to these patterns as modes of the resonator. Thus the modes and they periodicity are linked by the choice of resonator parameters.

This periodicity can be defined as the number of conventional round trips (double passes) required for any ray to return to an initial position and orientation, and can be found using geometrical ray analysis. If the Porro resonator matrix M is given by:

$$M = \begin{pmatrix} 1 & \frac{1}{2}L \\ 0 & 1 \end{pmatrix} \begin{pmatrix} 1 & 0 \\ -f^{-1} & 1 \end{pmatrix} \begin{pmatrix} 1 & 0 \\ -f^{-1} & 1 \end{pmatrix} \begin{pmatrix} 1 & L \\ 0 & 1 \end{pmatrix} \begin{pmatrix} 1 & 0 \\ -f^{-1} & 1 \end{pmatrix} \begin{pmatrix} 1 & 0 \\ -f^{-1} & 1 \end{pmatrix} \begin{pmatrix} 1 & \frac{1}{2}L \\ 0 & 1 \end{pmatrix}, \quad (5)$$

then an initial ray, which can be thought of as any element of a mode pattern, can be written as a two-row vector v_0 describing both the position and angular deviation of the ray. After p round trips through the resonator, v_0 will be transformed into a new vector v_p according to:

$$v_p = M^p v_0 = \sum_i \lambda_i^p \alpha_i \bar{v}_i, \quad (6)$$

where λ_i and \bar{v}_i are the eigenvalues and eigenvectors of the matrix M respectively and α_i are the coefficients required for the expansion of v_0 in terms of the eigenvectors. For repeatability of the mode we require $v_p = v_0$, found from the solution to the simultaneous equations (for each i) $\lambda_i^p = 1$.

This approach allows the periodicity of the cycling modes to be determined analytically, and compared to the periodic pattern observed in the spot size data from the numerical model. The results are illustrated graphically in Fig. 6, as well as in Table 1.

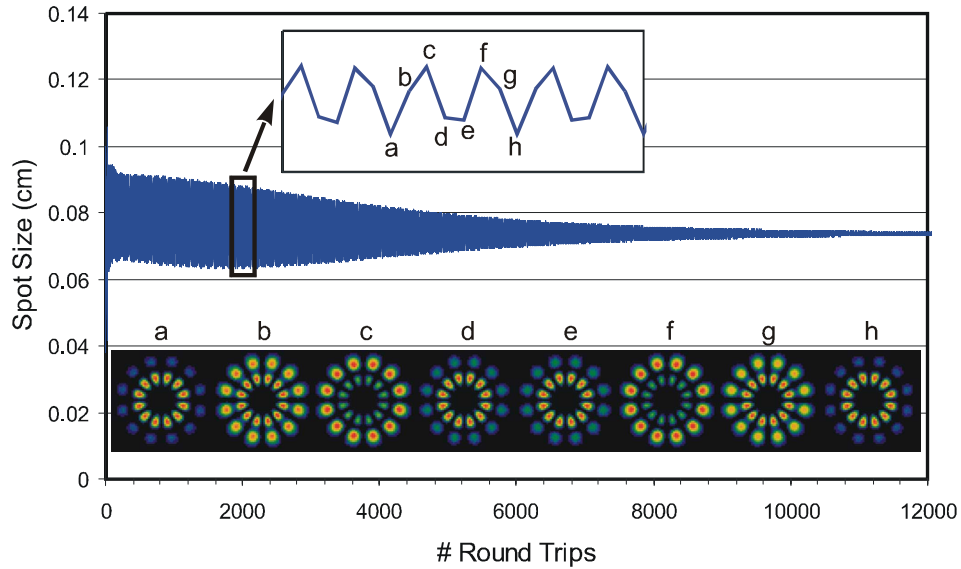


Fig. 6. Plot of spot size for 12 000 round trips (double passes) through a resonator with Porro angle 30° for $G = 0.9$, $N_F = 9.4$, illustrating the periodic nature of the spot size and showing eventual convergence. The sequence of modes through one period is also show.

Table 1. Periodicity comparison

G	p	
	Theory	Model
-1.0	none	none
0.0	none	none
0.5	3	3
0.707	4	4
0.809	5	5
0.867	6	6
0.9	7	7
0.924	8	8
0.94	9	9

Table 1 shows the agreement in periodicity predicted by geometric resonator theory compared to that observed in the numerical model for the beam loop modes. The numerical model also correctly predicts the higher order beam modes to have higher losses than the lower order petal-like mode. Because our numerical model allows the modes to oscillate indefinitely, loss selection ultimately results in the convergence of all starting fields to the petal-like patterns, as shown in Fig. 6 (see also Fig. 3 ‘large aperture mode’ movie). In the presence of gain and hence a limited build-up time, such a convergence would not necessarily take place.

It is pertinent at this point to discuss the possibility of the experimental observation of these complex beam patterns. Their losses are such that in a mode competing environment they are distinct from the petal-like patterns for a time period in the order of 1–2 μs , which is comparable to the mode build-up time of a typical actively Q-switched Porro prism laser (see Fig. 1). Thus while we cannot prove analytically that these complex beams are transverse modes of the resonator, their lifetime is such that it is very likely they are transverse modes, and there should be the possibility of observing them experimentally. There are however some limitations and technical challenges to such an experiment. It is likely that in a conventional linear standing wave resonator some combination of these modes might appear, and with a time averaged measurement a multi-mode pattern would be observed. We believe that we have already observed this.

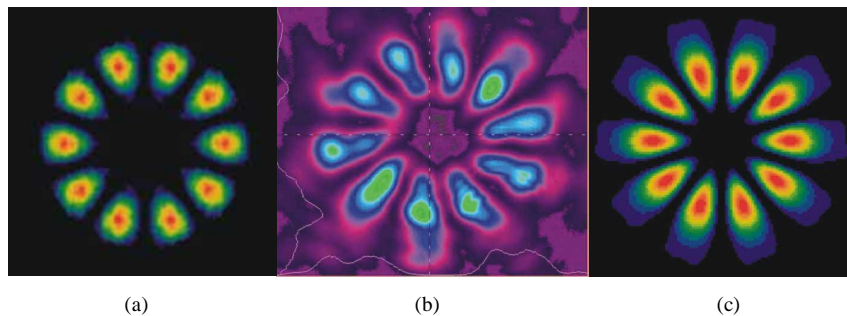


Fig. 7. (a) Petal mode, (b) Experimental beam pattern, (c) Average of 5 cycles of higher-order modes at 1000 round trips.

Figures 7 (a) – (b) shows the comparison of a previously calculated petal pattern together with experimental verification [6]. A time averaged output in the time period of the complex modes is shown in Fig. 7(c). Two observations can be made: firstly, the resulting pattern is again similar to a petal-like pattern, despite no petal-like mode component in the sequence, and secondly, the pattern shows an elongation of the energy distribution, and a departure from the compact petals seen in Fig. 7(a). The latter is more consistent with the experimentally observed pattern, which was measured on a stable resonator with large apertures. This suggests (but does not prove) that the complex modes we predict do indeed exist, and are

stable enough with low enough losses to be resonant in the cavity. In this sense they are likely to be viewed as higher order modes of the resonator.

So how to measure these modes? It is possible that the approach of others in selecting multi-pass modes might be employed, together with knowledge of our particular field distributions, as predicted in this work. It has been shown that either preferentially increasing the gain [8] or the loss [9] for a particular path can force oscillation of a particular multi-pass beam mode. The challenge is to adapt such approaches to mode selection in Porro prism resonators.

5. Kaleidoscope modes

The complex higher order modes revealed in the previous section (see movie link in Fig. 4 for more examples) show distinct similarities to so-called kaleidoscope modes [10,11]. The similarities are visual, which we acknowledge to be subjective given that such modes have not been put on a firm mathematical basis, but more important similarities exist in the generating mechanisms.

In [10] these field distributions were proposed as a result of the coherent superposition of n cosine gratings, each rotated with angular increments of $\psi = \pi/n$. The similarity between this and a rotating loss on the field at angles $\alpha = \pi/n$ (Eq. (1) with $i = 1$) in Porro prism resonators probably accounts for the likeness in output modes. In [11] kaleidoscope modes were generated using crossed apertures to sub-divide the input field to an axicon. This type of obstruction pattern is identical to the final loss field observed in Porro prism resonators (see Fig. 8 of [6]). While such fields were previously created external to the laser cavity, we have shown that the fundamental property of field sub-division in Porro prisms can produce similar fields directly from the laser cavity.

The generating mechanisms in both [10] and [11] have strong points of commonality with how intracavity Porro prisms are treated. However for completeness we must point out that the studies in question dealt with diffraction free beams created by plane waves traveling on cones, with no obvious link to our resonator. Despite this the output modes bear very strong likeness in form, and perhaps also in properties.

The ubiquitous nature of Porro prism resonators makes a study of such modes necessary in its own right, but there also exists the possibility of using such complex modes to excite complex photonic crystal structures, and so further study is required.

6. Conclusion

We have applied a previously developed mathematical model of intracavity Porro prisms to stable and unstable Porro prism resonators with large intracavity apertures. We have shown that higher order modes exist only if N_F is sufficiently large, and that these higher order modes closely resemble recently reported kaleidoscope modes due to the fundamental property of field sub-division in Porro prism resonators. The appearance of first the petal mode and then increasingly complex kaleidoscope modes with increasing aperture size leads to the conclusion that the petal-like modes are the lowest order modes of Porro prism resonators, while higher order modes exist in the form of kaleidoscope-like fields. We also predict that the standard petal mode is only observable from stable Porro prism resonators, and indicate how the stability criteria (G parameter) impacts on the cyclical nature of the higher order modes. We believe it is possible to observe these modes experimentally, but acknowledge that there are some technical challenges to overcome before doing so.

Acknowledgment

We would like to gratefully acknowledge the useful discussions and advice from Dr Christoph Bollig.